Scalable Computing: Practice and Experience, ISSN 1895-1767, http://www.scpe.org
© 2025 SCPE. Volume 26, Issues 2, pp. 916–923, DOI 10.12694/scpe.v26i2.4079

THE ENVIRONMENT PERCEPTION AND PATH PLANNING ALGORITHM FOR DRIVERLESS CARS BASED ON COMPUTER PROCESSING AND MULTI-SENSOR FUSION

YOUJIN ZHAO*

Abstract. This paper selects suitable sensors and equipment based on the characteristics of urban road traffic. Then, a multi-sensor information fusion system based on millimeter-wave radar/camera is established. In this way, the road traffic safety can be effectively controlled. Then, by improving D-S evidential reasoning, a "goal-decision" two-level information fusion method is established. Then, the multi-layer fusion experiment of multi-source sensing data under a tunnel environment is carried out. Experiments show that the ROI region correlation using camera and millimeter wave radar can improve the detection accuracy by 9.66%, effectively solving the limitations of single-sensor detection for automatic driving under complex conditions. The D-S evidential reasoning method processes the automatic driving sensor data. This reduces the false report rate of the sensor by 2.75%.

Key words: Tunnel environment; Driverless; Multi-sensing technology; D-S Principle of evidence; Goal - Determine the Layer 2 integration strategy.

1. Introduction. In recent years, due to the rapid development of artificial intelligence, its role in car driving is becoming increasingly apparent. This makes the car's operation on the road more efficient and safe. Driverless perception is the "eyes" of the car. At present, unmanned vehicles take the road surface as the main body, and the accuracy of their perception can meet most of the traffic monitoring requirements [1]. But most highways in China have underground tunnels at present. Its driving conditions are bad, noise interference is serious, and it is easy to cause the phenomenon of "missing detection" and "false detection" in driving. This causes traffic accidents inside the tunnel. However, the current domestic and foreign researches lack sufficient attention to the unmanned vehicles in the tunnel environment, and it is urgent to break through the problem of safety and reliability perception under this specific condition.

Some scholars use the D-S evidence principle and multi-sensor data for system fault diagnosis [2]. Some scholars have compared and studied the primary probability distribution from the perspectives of neural networks, Bayes and D-S. Some researchers have used SVM to solve fundamental probability assignment problems in D-S evidential reasoning and have applied it to practical fault diagnosis experiments. Some scholars add the unknown variable m(x) to the D-S evidence theory to reduce the contradiction between the evidence [3]. Some studies have used box-line and average substitution methods to detect and repair abnormal points and then used the adaptive weight fusion method for multilevel fusion of multiple sensor points of the same type. Finally, the D-S evidence information fusion method is adopted to solve the multi-objective coordination problem in complex scenes. Some scholars have studied improved D-S evidence reasoning methods to overcome the severe contradictions in the existing methods [4]. This project intends to use the D-S evidence theory to optimize it. Then, the multi-dimensional information fusion method is designed. This project will effectively integrate multi-source sensor data at the target layer and the decision layer, which can obtain accurate information and lay a foundation for the application of vehicle control decision-making, autonomous obstacle avoidance, path planning and other aspects.

2. Design of automatic driving tunnel environment awareness system. Given the poor lighting conditions and instability of unmanned driving in underground traffic, it is necessary to carry out a unique design of its hardware [5]. Considering the tunnel's specific working conditions and the sensor's hardware characteristics, a collaborative sensing and identification method based on millimeter-wave radar and camera is

*Department of Automobile Engineering, Anhui Automobile Vocational and Technical College, Hefei 230601, China (ahqczyjsxy@163.com)

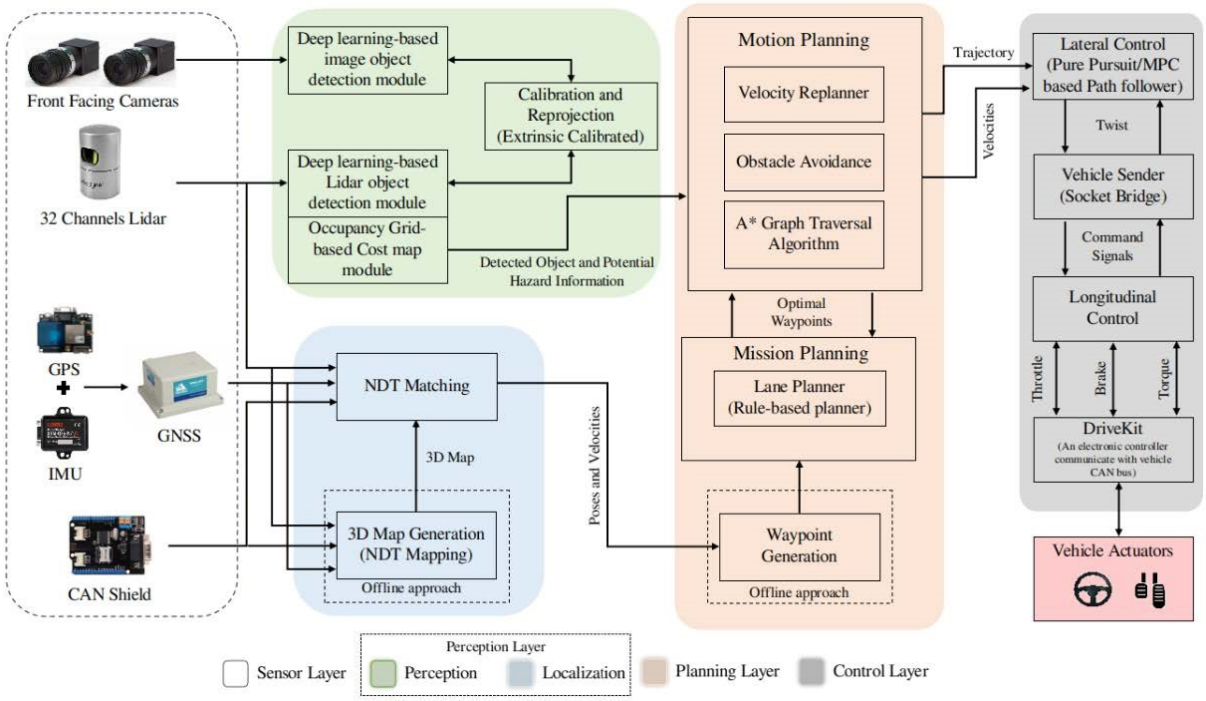

Fig. 2.1: Architecture of unmanned multi-sensor fusion sensing system.

proposed [6]. In addition, multiple ultrasonic radars can be set around the vehicle body to achieve the purpose of short-range collision avoidance. The layout scheme of the multi-sensor sensing System for unmanned vehicles is shown in Figure 2.1 (the picture is quoted in System, Design and Experimental Validation of Autonomous Vehicle in an Unconstrained Environment).

2.1. Goal-decision two-level information fusion strategy. For the specific driving scene of the tunnel, selecting the appropriate sensor and layout is the fundamental guarantee of obtaining efficient detection information. An efficient calculation method for sensing information is designed to achieve accurate detection [7]. Then, post-processing based on the data collected by multiple sensors is the key to improving detection accuracy.

2.1.1. Two-layer information fusion induction method. A reasonable information fusion method using multiple sensors is proposed. First, the ultrasonic sensor has some problems, such as small range and difficulty locating obstacles, and the fusion of multi-sensor information is directly related to the accuracy of recognition results. Secondly, the diversity of the detection environment leads to the scattered arrangement of ultrasonic sensors, and there is no compelling data fusion [8]. Therefore, the design of this paper only plays the role of collision avoidance alarm.

This paper proposes a fusion algorithm based on the target layer. That is the feature and decision fusion algorithms [9]. Because of the light conditions in the tunnel, the information obtained is more complicated than the road conditions on the ground. Therefore, data loss should be reduced as much as possible to ensure data quality. This project intends to study the information fusion method at two ”target layer - decision layer” levels for unmanned vehicles in tunnels. Its data Fusion process is shown in Figure 2.2 (image cited in Sensor Fusion for Radar Detection).

2.1.2. Information fusion model of two-layer perceptron. This paper proposes a two-layer information fusion model based on the ”target layer - decision layer.” This project uses millimeter-wave radar and a camera as the hardware platform for integration [10]. The fusion of target layer and decision layer and the final

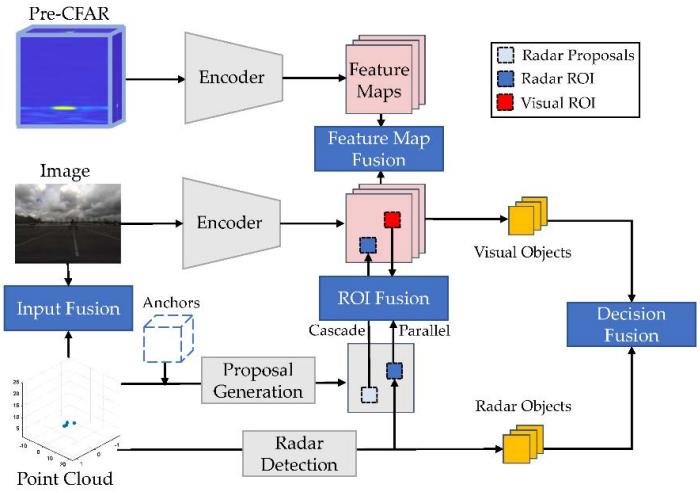

Fig. 2.2: Two-layer fusion strategy based on millimeter wave and camera.

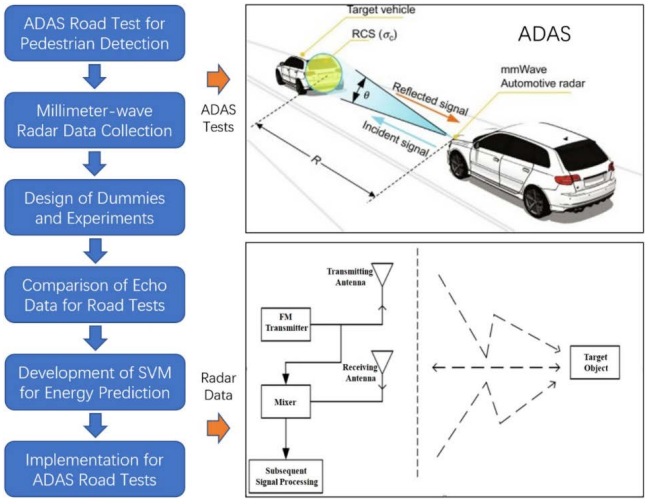

Fig. 2.3: Two-level information fusion model of millimeter wave radar and camera.

result output are realized through the acquisition and processing of multiple sensors. First, the camera detects objects, forming two types of sensing areas. Secondly, the correlation analysis of the two categories of interest regions is carried out and compared with the threshold. In this way, the Adaboost quadratic discriminant method is adopted. Finally, through the D-S theory of evidence, Obtain the motion state of an unmanned vehicle (Figure 2.3 cited in Using millimeter-wave radar to evaluate the performance of dummy models for advanced driving) assistance systems test).

D-S evidence theory has lower prior requirements. It has significant advantages in dealing with uncertain information such as combination and decision [11]. The Adaboost method uses weighted changes to train and learn the primary classifier and then uses different sampling weights to complete the kernel of multiple classifiers (Figure 2.4). This is to reduce the weight of the correct and wrong samples so that the following classification will focus on identifying the problematic samples. It improves classification accuracy by reclassifying new training samples with existing weights. It combines all classifiers according to some criteria to form a new

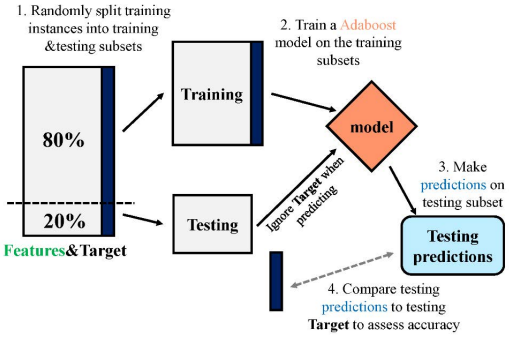

Fig. 2.4: Overall flow chart of Adaboost algorithm.

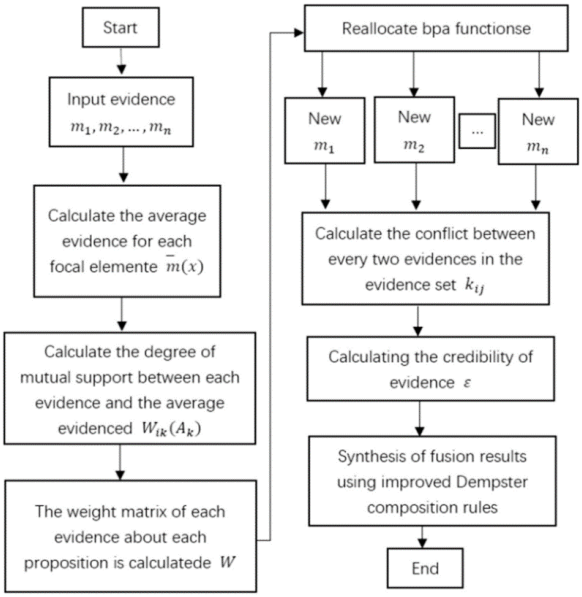

Fig. 2.5: D-S evidence fusion process diagram.

robust classifier, the final decision classifier.

2.2. The basic probability is reconfigured by constructing an evidence vector. The principal diagram of the D-S evidence fusion process based on multi-source information is shown in Figure 2.5. It fully uses the advantages of various sensors to detect the distance and Angle of obstacles ahead through vision and millimeter wave radar [12]. The D-S evidence theory comprehensive criterion is used to fuse multi-source information and judge the final fusion effect.

Define the identity frame as $F = \{B_1, B_2, B_3, \ldots, B_n\}$. Let's call $H_i = [h_i(B_1), h_i(B_2), \ldots, h_i(B_n)]^T$ the evidence vector. The element $h_i(B_j)$ in the evidence vector H_i represents the confidence of class j provided by sensor i. Here $i = 1, 2, \ldots, m; j = 1, 2, \ldots, n$; So, the evidence set is $HH = \{H_1, H_2, H_3, \ldots, H_m\}$. Construct the distance A between the evidence vectors. The distance of the vectors is the degree of directional deviation between the two vectors [13]. This paper uses the Pearson correlation coefficient to characterize the distance between two evidence vectors. Compared with cosine similarity, the Pearson correlation coefficient can prevent error interference when the vector only shifts. It can measure the difference between two spatial vector individuals well.

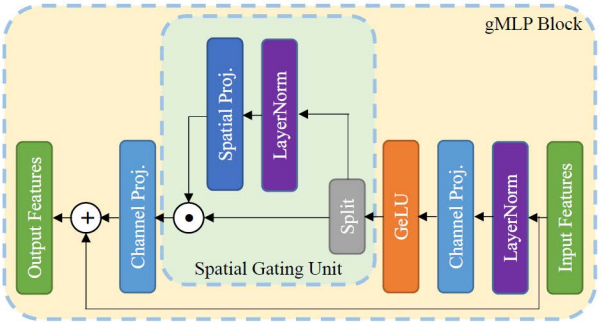

Fig. 3.1: Radar wave detection road surface model.

The distance $s_{\alpha\beta}$ between the two vectors is constructed, which is the directional deviation between the two vectors. This paper uses the Pearson correlation coefficient to characterize the distance between two evidence vectors. This method overcomes the error of the traditional feature extraction method based on wavelet transform. It's an excellent way to measure the difference between two vectors. Under the identification framework $F = \{B_1, B_2, B_3, \ldots, B_n\}$, the distance $s_{\alpha\beta}$ between evidence H_α and H_β is determined by equation (2.1), where $H_\alpha, H_\beta \in HH$:

$$\begin{aligned} s_{\alpha\beta} &= e^{1-\varrho(H_\alpha, H_\beta)} \\ Q\left(H_\alpha, H_\beta\right) &= \frac{\operatorname{Cov}\left(H_\alpha, H_\beta\right)}{\sqrt{\operatorname{Var}\left[H_\alpha\right] \operatorname{Var}\left[H_\beta\right]}} \\ &= \frac{h \sum_{r=1}^{m} h_\alpha\left(B_r\right) h_\beta\left(B_r\right) - \sum_{r=1}^{m} h_\alpha\left(B_r\right) h_\beta\left(B_r\right)}{\sqrt{\sum_{r=1}^{m} h_\alpha^2\left(B_r\right) - \left(\sum_{r=1}^{m} h_\alpha\left(B_r\right)\right)^2} \sqrt{\sum_{r=1}^{m} h_\beta^2\left(B_r\right) - \left(\sum_{r=1}^{m} h_\beta\left(B_r\right)\right)^2}} \end{aligned} \tag{2.1}$$

The evidence weighting factor $\eta\left(H_\alpha\right)$ was determined. The model is used to characterize the importance of the corresponding evidence information H_α in the image. The weighted assignment factor $\eta\left(H_\alpha\right)$ during the final fusion processing is:

$$\eta\left(H_\alpha\right) = \left[1 - in\left(H_\alpha\right)\right] e^{-in\left(H_\alpha\right)} \tag{2.2}$$

3. Low-resolution tunnel identification under multi-sensor information fusion.

3.1. Uncertainty in tunnel detection by radar wave. Millimeter wave radar has the advantages of strong anti-interference, good penetration and high detection resolution. It is suitable for monitoring the road environment throughout the day and is a powerful aid to road perception and detection [14]. Through the analysis of the damaged road surface pits, the concrete steps of detecting the road surface with radar waves are described (Figure 3.1).

When the radar sends out multiple beams to detect the road, the middle component wave in Figure 3.1 deflects outward from the bottom of the pit to form an effective wave. Bounce off the ground and back onto the radar. Multiple pulse signals emitted by radar are processed. The damaged road surface topography can be detected using the residual signal and the actual signal [15]. When the distance between two rays on the boundary of the damaged road is L, and the Angle between one ray and the ground is ζ, which can be calculated by the phase difference between the echo signals received by the radar, and the depth is h, then the value of 1 can be measured and calculated by using the lost waste wave. Then, the irradiation relation shown in Figure 3.1 can be obtained:

$$\begin{cases} h = \frac{l+\Delta\tau}{\sin(\zeta \pm \Delta\omega)} \\ h > \frac{l+\Delta\tau}{\cos(\zeta \pm \Delta\omega)} \end{cases} \tag{3.1}$$

$\Delta\omega$ represents the radar's sweep Angle deviation, ω represents the measurement error, and h represents the size of the crater on the damaged road surface. Its value can be calculated according to the minimum values measured [16]. It can construct a road recognition system based on radar waves.

3.2. Sensor information fusion strategy. Assuming that the boundary detected by vision and radar wave detectors is U_{cam} and u_{rad} , the overlapping area of the two boundaries is R_j, and the area of the two boundaries is R_h, then the intersection ratio of the IOU is:

$$IOU = \frac{R_j}{R_h} \tag{3.2}$$

If the IOU in Formula 3.2 is 0.6 to 1 , it can be determined that both the camera and the radar wave have detected the road, and the measurement data of both are verified and consistent. It has high credibility. If A suitable number is not found, then the global neighbor algorithm is used to conduct data correlation, set the radar and camera failed to match the target point m, n, their distance to the specified point l_r, l_c, according to the distance between the position and the coordinate point, according to this number to arrange the coordinate, you can obtain the vision and radar target point matrix T, U. The residual amount of the radar and camera detection points at the time u is denoting $\xi_{ij}(u)$. It can be expressed by the formula (3.3):

$$\xi_{ij}(u) = \Xi_j(u) - HR_i(u) \tag{3.3}$$

H stands for state transfer matrix, The standardized distance from the camera detection point j to the radar detection point. The following formula can express me

$${l^2}_{ij} = {\Xi^T}_{ij}(u) R_{ij}^{-1}(u) \xi_{ij}(u) \tag{3.4}$$

$R_{ij}^{-1}(u)$ represents the covariance matrix of $\xi_{ij}(u)$.F_i is the threshold of radar detection point i. If the normalized distance is not greater than the threshold, it indicates that the camera detection point is in the coverage area of the radar detection point. They can work together [17]. Each radar detection point corresponds to the camera detection point. The cost distribution in the GNN algorithm is as follows

$$\Phi_{ij} = \begin{cases} l_{ij}^2, l_{ij}^2 \leq F_i \\ F_i, l_{lj}^2 > F_i \end{cases} \tag{3.5}$$

The docking and matching point cloud data on the unpaved road are realized by solving the cost equation. Then, the radar and camera perception data are organically combined.

4. Vehicle fusion perception test in a tunnel environment.

4.1. Identification parameter setting. First, set up the buffer queue system. Because the camera's frame rate selected in this paper is 30 FPS, and the maximum detection range is 60 meters. Setting a buffer time of 30 frames at a time can also ensure driving safety. When an accident occurs during data fusion, the ultrasonic radar's proximity collision avoidance command can be immediately transmitted to the industrial control computer, and an emergency stop command can be executed [18]. It guarantees the safety of the vehicle. A basic probability distribution model based on D-S evidence theory is proposed. Then, in groups of 20 frames, each level of data is gradually entered into the cache. The D-S evidential reasoning method is used to combine the criteria to achieve the purpose of enhancing the detection accuracy. Finally, data such as target type, relative position and relative speed are obtained.

4.2. Test results and analysis. This project selects 20 indicators found in the actual road operation as the research object to test the application effect of the two-layer information fusion method of "target layer + decision layer" in the actual traffic scene. The fusion results of environmental perception in two stages of tunnel testing are shown in Table 4.1. By studying the "target layer and decision layer" fusion, the information fusion between millimeter wave and image can be accomplished efficiently under practical test conditions. In this way, objects in the line of sight can be accurately detected and obtain status information.

Table 4.1: Results of a two-stage perception test in a tunnel.

Target ID	Longitudinal coordinates (m)	Lateral coordinates (m)	Longitudinal relative velocity (m/s)	Lateral relative velocity (m/s)	Target level fusion results
1	24.146	-0.729	6.281	0.010	car/0.80
2	11.208	0.542	-8.552	0.000	person/0.87
3	16.073	-0.708	5.333	0.000	car/0.88
4	11.021	-0.719	1.219	0.000	car/0.87
5	49.927	-0.729	8.115	0.010	car/0.38
6	18.417	-0.646	4.469	0.010	car/0.77
7	32.521	-0.490	5.646	0.000	truck/0.44
8	32.156	-0.552	4.802	0.021	car/0.77
9	36.740	-0.302	3.490	0.010	car/0.88
10	19.875	-0.583	6.229	0.019	car/0.77
11	28.479	0.500	-8.510	0.000	car/0.41
12	73.708	-0.500	3.271	0.010	car/0.85
13	45.469	-0.521	1.854	0.010	car/0.84
14	6.396	-0.490	3.760	0.021	car/0.73
15	19.198	-0.438	6.135	0.010	car/0.74
16	53.125	0.021	10.125	0.000	sign/0.47
17	19.490	-0.677	5.396	0.010	car/0.78
18	21.760	-0.417	6.979	0.010	car/0.77
19	14.917	-0.500	6.406	0.000	car/0.57
20	38.729	-0.448	8.125	0.000	car/0.77

5. Conclusion. According to the characteristics of the current tunnel unmanned vehicle environment, the approach to improve the accuracy of intelligent perception of unmanned driving is studied from the perspectives of hardware selection, layout and information fusion. The experimental platform of the experimental vehicle was constructed, and the underground tunnel with suitable lighting was selected as the experimental site for experimental testing. Experimental results show that this method can improve the image detection accuracy by 9.66%. It can solve the problem that the traditional camera has poor visual perception ability in the roadway. The image information fusion method based on the decision layer proposed in this project will effectively reduce the false reports of images. So, the detection ability of tunnel images is improved effectively.

REFERENCES

[1] Li, Q., Queralta, J. P., Gia, T. N., Zou, Z., & Westerlund, T. (2020). Multi-sensor fusion for navigation and mapping in autonomous vehicles: Accurate localization in urban environments. Unmanned Systems, 8(3), 229-237.
[2] Natan, O., & Miura, J. (2022). Towards compact autonomous driving perception with balanced learning and multi-sensor fusion. IEEE Transactions on Intelligent Transportation Systems, 23(9), 16249-16266.
[3] Yang, P., Duan, D., Chen, C., Cheng, X., & Yang, L. (2020). Multi-sensor multi-vehicle (MSMV) localization and mobility tracking for autonomous driving. IEEE Transactions on Vehicular Technology, 69(12), 14355-14364.
[4] Yi, C., Zhang, K., & Peng, N. (2019). A multi-sensor fusion and object tracking algorithm for self-driving vehicles. Proceedings of the Institution of Mechanical Engineers, Part D: Journal of automobile engineering, 233(9), 2293-2300.
[5] Rick, M., Clemens, J., Sommer, L., Folkers, A., Schill, K., & Büskens, C. (2019). Autonomous driving based on nonlinear model predictive control and multi-sensor fusion. IFAC-PapersOnLine, 52(8), 182-187.
[6] Wang, K., Cao, C., Ma, S., & Ren, F. (2021). An optimization-based multi-sensor fusion approach towards global drift-free motion estimation. IEEE Sensors Journal, 21(10), 12228-12235.
[7] Kovacova, M., Oláh, J., Popp, J., & Nica, E. (2022). The algorithmic governance of autonomous driving behaviors: Multi-sensor data fusion, spatial computing technologies, and movement tracking tools. Contemporary Readings in Law and Social Justice, 14(2), 27-45.
[8] Lian, H., Pei, X., & Guo, X. (2020). A local environment model based on multi-sensor perception for intelligent vehicles. IEEE Sensors Journal, 21(14), 15427-15436.
[9] Tao, X., Zhu, B., Xuan, S., Zhao, J., Jiang, H., Du, J., & Deng, W. (2021). A multi-sensor fusion positioning strategy for intelligent vehicles using global pose graph optimization. IEEE transactions on vehicular technology, 71(3), 2614-2627.

[10] Osman, M., Mehrez, M. W., Daoud, M. A., Hussein, A., Jeon, S., & Melek, W. (2021). A generic multi-sensor fusion scheme for localization of autonomous platforms using moving horizon estimation. Transactions of the Institute of Measurement and Control, 43(15), 3413-3427.
[11] Zhang, S., Zhao, X., Lei, W., Yu, Q., & Wang, Y. (2020). Front vehicle detection based on multi-sensor fusion for autonomous vehicle. Journal of Intelligent & Fuzzy Systems, 38(1), 365-377.
[12] Weon, I. S., & Lee, S. G. (2019). Environment recognition based on multi-sensor fusion for autonomous driving vehicles. Journal of Institute of Control, Robotics and Systems, 25(2), 125-131.
[13] Liu, Z., Xiao, G., Liu, H., & Wei, H. (2022). Multi-sensor measurement and data fusion. IEEE Instrumentation & Measurement Magazine, 25(1), 28-36.
[14] Jung, R., & Weiss, S. (2021). Modular multi-sensor fusion: A collaborative state estimation perspective. IEEE Robotics and Automation Letters, 6(4), 6891-6898.
[15] Yin, R., Cheng, Y., Wu, H., Song, Y., Yu, B., & Niu, R. (2020). Fusionlane: Multi-sensor fusion for lane marking semantic segmentation using deep neural networks. IEEE Transactions on Intelligent Transportation Systems, 23(2), 1543-1553.
[16] Cui, Y., Chen, R., Chu, W., Chen, L., Tian, D., Li, Y., & Cao, D. (2021). Deep learning for image and point cloud fusion in autonomous driving: A review. IEEE Transactions on Intelligent Transportation Systems, 23(2), 722-739.
[17] Li, A., Zheng, B., & Li, L. (2020). Intelligent transportation application and analysis for multi-sensor information fusion of Internet of Things. IEEE Sensors Journal, 21(22), 25035-25042.
[18] Ravindran, R., Santora, M. J., & Jamali, M. M. (2020). Multi-object detection and tracking, based on DNN, for autonomous vehicles: A review. IEEE Sensors Journal, 21(5), 5668-5677.

Edited by: Hailong Li
Special issue on: Deep Learning in Healthcare
Received: May 31, 2024
Accepted: Jul 5, 2024